Interlayer tunnelling spectroscopy of the charge density wave state in $NbSe_3$

2003 J. Phys. A: Math. Gen. 36 9323

(http://iopscience.iop.org/0305-4470/36/35/317)

INSTITUTE OF PHYSICS PUBLISHING JOURNAL OF PHYSICS A: MATHEMATICAL AND GENERAL

J. Phys. A: Math. Gen. **36** (2003) 9323–9335 PII: S0305-4470(03)59499-9

Interlayer tunnelling spectroscopy of the charge density wave state in $NbSe_3$

Yu I Latyshev[1,2], P Monceau[2,3], A A Sinchenko[4], L N Bulaevskii[5], S A Brazovskii[6], T Kawae[7] and T Yamashita[7,8]

[1] Institute of Radio-Engineering and Electronics RAS, Mokhovaya 11-7, 101999 Moscow, Russia
[2] CRTBT-CNRS, BP 166, 38042 Grenoble, France
[3] Laboratoire Leon Brillouin, CEA-CNRS, CEA Saclay, 91191 Gif-sur-Yvette, France
[4] Moscow Engineering-Physics Institute, 115409 Moscow, Russia
[5] Los Alamos National Laboratory, Los Alamos, NM 87545, USA
[6] LPTMS-CNRS, Universite Paris-Sud, 91405 Orsay, France
[7] RIEC, Tohoku University, 980-8577 Sendai, Japan
[8] NICHE, Tohoku University, 980-8577 Sendai, Japan

Received 11 February 2003, in final form 9 May 2003
Published 20 August 2003
Online at stacks.iop.org/JPhysA/36/9323

Abstract

Using small staked junctions of high quality we have measured interlayer tunnelling spectra of the layered quasi-one-dimensional material $NbSe_3$. We identified a number of new features in the spectra: zero bias conductance peak (ZBCP), charge density wave (CDW) gap structure for lower and upper CDW, the sub-gap structure inside the CDW gap. The ZBCP dominates in low-temperature spectra. We discuss its origin as being related to the interlayer coherent tunnelling of the carriers uncondensed into CDW. We found that ZBCP is sensitive to magnetic field and its orientation. The field perpendicular to the layers broadens ZBCP while the parallel field narrows it. We consider the sub-gap structure as associated with self-localized states inside the gap.

PACS numbers: 42.25.Gy, 71.45.Lr, 72.15.Nj, 74.25.Gz

1. Introduction

The method of interlayer tunnelling is based on the layered crystalline structure of some highly anisotropic materials where elementary, atomically thin conducting layers are separated by elementary isolating layers. The transport along the layers in these materials is provided by metallic intralayer conductivity while the transport across the layers occurs via interlayer tunnelling. If the metallic layer undergoes at low temperatures a phase transition into an electron condensed state (e.g. a superconducting or magnetic state) the interlayer tunnelling may be used as an effective tool to study that state. This method has been effectively realized in layered cuprate superconductors. The interlayer tunnelling of Cooper pairs (the so-called

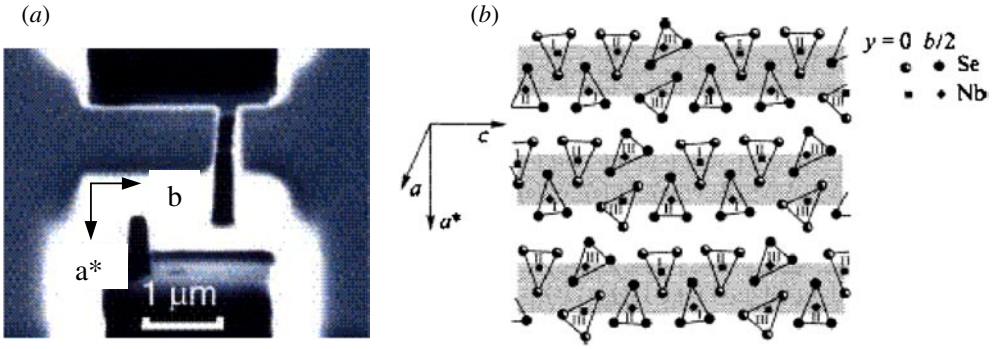

Figure 1. (*a*) The SIM image of the $NbSe_3$ stack fabricated by the FIB technique. (*b*) Schematic representation of the $NbSe_3$ crystalline structure in the *ac*-plane. Conducting planes are indicated by shading.

intrinsic Josephson effect) [1] and quasiparticles [2] has been successfully demonstrated. Valuable information about the superconducting energy gap and pseudogap [3] symmetry of the order parameter [2], coherency of interlayer tunnelling [4], etc has been obtained by this method. One of the attractive features of the method compared with some other widely used spectroscopic techniques such as IRS, ARPES, STM is the possibility of getting information from the bulk of the material.

Recently, the method has been extended to other types of layered materials such as layered manganites [5] and layered CDW materials [6, 7]. Here we report on detailed studies of the interlayer tunnelling spectra of CDW conductor $NbSe_3$. To compare with previous investigations [6, 7] the present experiments were carried out on much more perfect stacked structures; they cover a wider temperature range 4.2–164 K and include measurements in high magnetic fields. This allowed us to reveal a number of new features of CDW spectroscopy in $NbSe_3$.

2. Stacked structure fabrication and characterization

$NbSe_3$ stacks have been fabricated by the focused ion beam (FIB) technique described in [8]. At the first stage a thin $NbSe_3$ whisker with a thickness of about 1 μm was fixed by its wider *bc*-face to a crystalline quartz substrate and glued by 1% solution of collodion in amylacetate. The top surface of the sample was then cleaned by oxygen plasma and four probes were attached by indium. The distance between the inner potential probes was less than 100 μm. At the second stage, the sample was narrowed by a FIB to form a micro-bridge in the *bc*-plane with sizes $L_b \times L_c = 3\ \mu\text{m} \times 1\ \mu\text{m}$, then a sample was turned by 90° around the *b*-axis and two narrow cuts made perpendicular to the a^*b-face of the bridge (see figure 1(*a*)) to form overlap structure. The spacing between the cuts along the *b*-axis was 1 μm and the overlap length between the ends of the cuts along a^*-axis was 0.03–0.05 μm. The micrograph of the structure obtained is shown in figure 1(*a*). Typical sizes were $L_{a^*} \times L_b \times L_c = 0.03\ \mu\text{m} \times 1\ \mu\text{m} \times 1\ \mu\text{m}$.

To confirm the results obtained on stacked structures, part of the measurements was also carried out on point contacts $NbSe_3$–$NbSe_3$ formed along the a^*-axis [7]. The *I–V* characteristics were measured by 4-probes with computer controllable current source and nanovoltmeter. The $R(T)$ characteristics were measured at small ac current by a phase sensitive bridge. For a geometry of the structures we used most of the voltage measured

Table 1. Parameters of the $NbSe_3$ stacked junctions.

No	L_b (μm)	L_c (μm)	R (4.2 K) (Ω)	$R(300)/R(4.2)$	ZBCP (height/bg.@4.2 K)
4-3	1.0	1.0	2.9	20	27
5-6	1.0	1.0	4.0	17	24

between potential probe drops on the stack across the layers. We estimate the contribution of the electrode parts of the crystal attached to the stack to be less than 5%. A magnetic field up to 8.5 T was supplied by a superconducting coil, while stronger fields up to 20 T were supplied by the Bitter coil in the Laboratory of High Magnetic Fields, Grenoble.

The geometry of the structures we used is convenient for direct measurements of resistivity across the layers, ρ_{a^*}, in $NbSe_3$. By measuring a number of structures we found ρ_{a^*} to be 0.1–0.2 Ω cm at room temperature. That implies very high interlayer conductivity anisotropy $\sigma_{a^*}/\sigma_b \sim 10^{-3}$ compared with intralayer anisotropy $\sigma_c/\sigma_b \sim 10^{-1}$ [9]. One can then suggest that similarly to the layered high-T_c superconductors, the conductivity in $NbSe_3$ is localized in highly conducting atomic layers well isolated from each other. These elementary layers have been identified from the analysis of crystalline structure of $NbSe_3$ [7]. As was shown, the elementary prisms in the *bc*-plane are assembled into coupled bi-layers where prism edges are oriented and shifted towards each other. That provides conducting layers with higher density of conducting chains (shaded layers in figure 1(*b*)), while the neighbouring conducting layers are separated by a double barrier of insulating prism bases.

It has been suggested [7] that the electron condensation into CDW occurs mostly in the elementary conducting layers. That results in the modulation of the amplitude of the CDW order parameter across the layers providing the possibility of interlayer tunnelling as in layered high-T_c superconductors.

The quality of stacked structures may be characterized by the residual resistivity ratio $\rho_{a^*}(300\ \mathrm{K})/\rho_{a^*}(4.2\ \mathrm{K})$ and by the presence of ZBCP at low temperatures [7]. The data reported below are mainly on $NbSe_3$ stacks #4-3, and #5-6 of the best quality and have also been reproduced for four more samples. The high quality samples we studied had $\rho_{a^*}(300\ \mathrm{K})/\rho_{a^*}(4.2\ \mathrm{K}) \approx 20$ and sharp ZBCP with the amplitude to background ratio at 4.2 K $\sim$30 (see table 1). Typical $\rho_{a^*}(T)$ dependence resembles the temperature dependence for in-plane resistivity $\rho_b(T)$. However, in the normal state (above Peierls transitions) $\rho_{a^*}(T)$ drops on cooling much slower in comparison with normalized in-plane resistivity (figure 2). Similar behaviour is known in layered high-T_c materials above T_c (see inset to figure 2). Also the out-of-plane residual resistivity ratio is three to four times less than the in-plane one even for the best samples. That means that conductivity anisotropy σ_b/σ_{a^*} significantly increases at low temperatures.

3. Temperature evolution of interlayer tunnelling spectra

Figure 3(*a*) shows interlayer tunnelling spectrum $\mathrm{d}I/\mathrm{d}V$ versus V of $NbSe_3$ stack #4-3 at 4.2 K. One can clearly see the symmetric structure of peaks. The highest peak corresponds to zero bias, i.e. ZBCP. Two other peaks at $V_1 = \pm 120$ mV and $V_2 = \pm 50$ mV are also very sharp and may be clearly distinguished directly from the *I–V* characteristics (figure 3(*b*)). The position of the peaks is close to the double gap values for the upper and lower CDW gaps known from the STM measurements [10]: $\Delta_2 = 25$–35 meV, $\Delta_1 = 60$–100 meV. We can

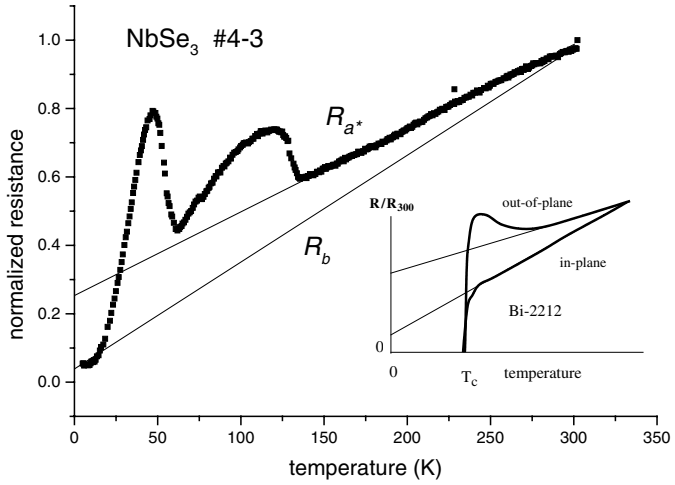

Figure 2. Normalized $R_{a^*}(T)/R_{a^*}(300)$ dependence for $NbSe_3$ stack #4-3. Straight lines show normalized metallic behaviour for the out-of-plane (R_{a^*}) and in-plane (R_b) dependences extrapolated to zero temperature. The insert schematically shows the similar difference of in-plane and out-of-plane metallic behaviour for Bi-2212.

therefore identify them as $eV_1 = 2\Delta_1$, $eV_2 = 2\Delta_2$. To verify that we have studied temperature evolution of the spectra (figure 4) and found that the peak at V_2 indeed disappears at temperature corresponding to lower Peierls transition T_{p2}, and the peak at V_1 disappears at $T > T_{p1}$. Thus we can conclude that at low temperatures below T_{p2} both CDWs coexist independently.

ZBCP evolves with temperature in the following way. First, the ZBCP amplitude remains nearly unchanged up to 8 K then gradually drops and finally ZBCP disappears above 25 K (figure 4(*b*)). The spectrum above 25 K becomes of tunnelling type. Its characteristic feature is a sharp increase of tunnelling conductance above some threshold voltage, while the voltage of maximum increase, V_0, scales with the gap voltage $2\Delta_2$ as $2\Delta_2/eV_0 \approx 3$. Just above the lower Peierls transition we see again broad ZBCP (figure 4(*c*)), ten times broader than the lower ZBCP and with an amplitude 20 times less than the low-temperature ZBCP. However, that evolves with increasing temperature in a very similar way to the lower one.

The main features of the interlayer tunnelling have also been reproduced on point contacts $NbSe_3/NbSe_3$ formed along the a^*-axis (figure 5(*a*)). It should be noted that ZBCP observation is closely related to a quality of the structure. The more perfect the structure the higher and sharper the ZBCP is. For the best stacks the ratio of ZBCP amplitude to background reached 20, while for point contacts it was 2–6. For point contacts of poor quality ZBCP can be absent. Figure 5(*b*) shows that ZBCP disappears with contact quality degradation after many touches.

We consider that Joule self-heating does not affect essentially the gap structures observed. In fact, we did not find any considerable changes in the peak position for stack resistance variation from 10 to 50 Ω and even for bigger variation in resistance of point contacts within 10–200 Ω. As was demonstrated for BSCCO stacks, self-heating effects can be significantly reduced with a decrease of lateral sizes down to micron scale [11, 12]. That was one of the reasons for using micron-sized $NbSe_3$ stacks for interlayer spectroscopy.

Figure 6 shows that temperature dependence of both CDW gaps follows the BCS theory well. The deviation below 25 K occurs when ZBCP dominates in the spectra, probably, because of some effective coalescence of the gap peaks with ZBCP. The fitted CDW gaps at low temperatures are $2\Delta_2 = 60$ mV, $2\Delta_1 = 140$ mV.

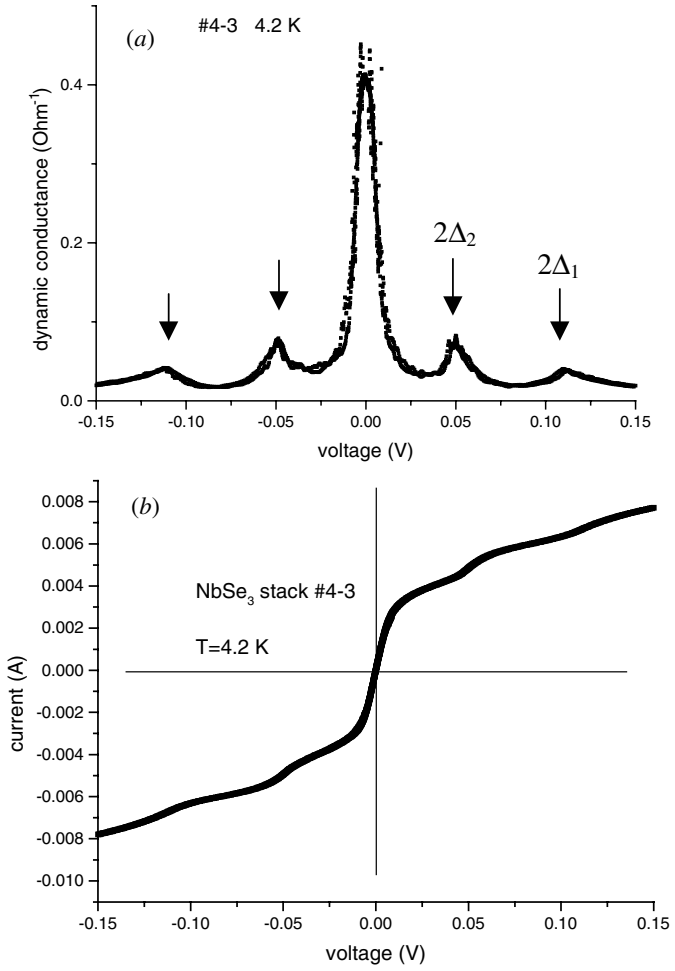

Figure 3. Interlayer tunnelling spectrum and the *I–V* characteristic of $NbSe_3$ stack #4-3 at 4.2 K.

4. Discussion: ZBCP and gap structure

The theoretical model developed by Bulaevskii [7] considers ZBCP a result of coherent interlayer tunnelling of the charge carriers localized in the pockets (ungapped parts of the Fermi surface). Coherent tunnelling implies the conservation of the particle in-plane momentum in the process of tunnelling. This condition is necessary because the pockets represent some localized small parts of the Fermi surface and electron momentum should not be scattered beyond the pockets by tunnelling from one layer to another. In this case the interlayer tunnelling *I–V* characteristic for $eV < 2\Delta$ is expressed as follows [7]:

$$I(V) = \frac{N(0)|t|^2\gamma eV}{2\pi^3(e^2V^2 + 4\gamma^2)} \tag{1}$$

where $N(0)$ is the density of states in the pockets, t is the matrix element for the interlayer tunnelling with momentum conservation, $\gamma = \hbar\nu$ and ν is the collision frequency. Here temperature-dependent γ accounts for the energy uncertainty for the state characterized by the momentum $\mathbf{p}$. The value of γ is determined by two channels, the intralayer scattering,

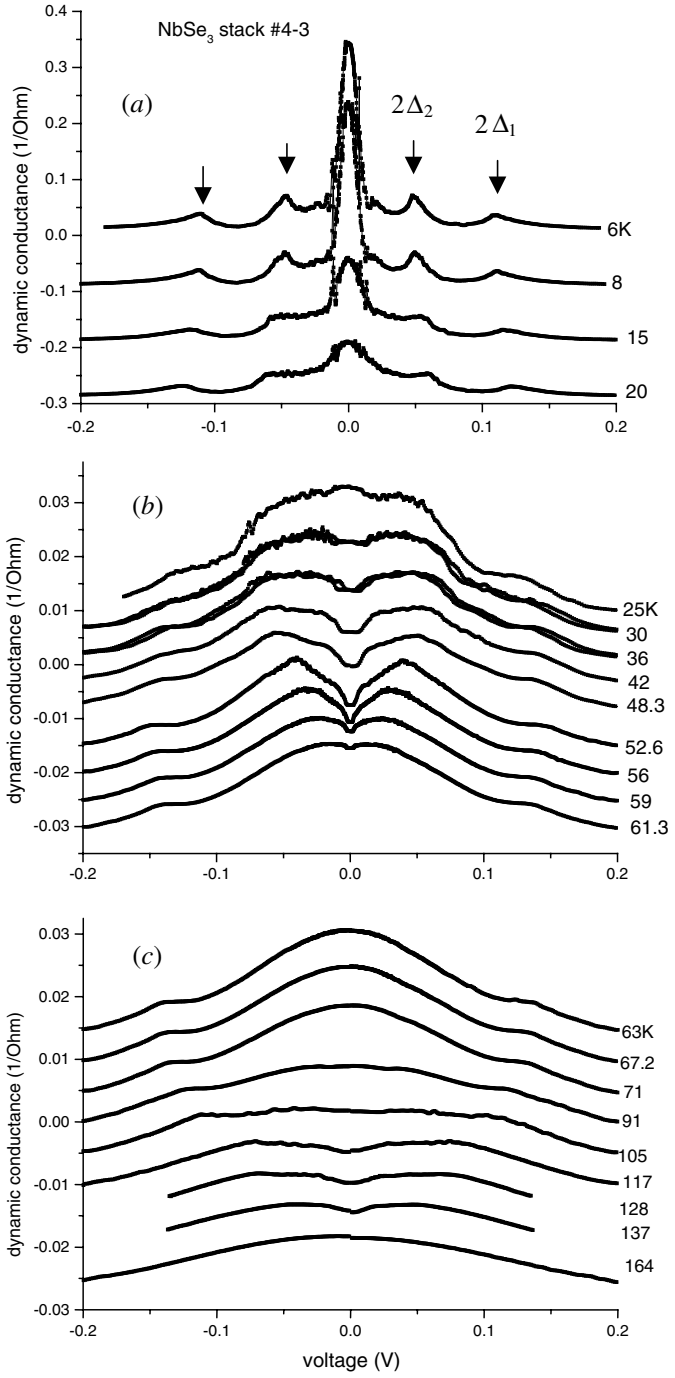

Figure 4. Temperature evolution of interlayer tunnelling spectra $\mathrm{d}I/\mathrm{d}V(V)$ in three temperature intervals. Curves are vertically shifted for clarity. The scale for each interval relates to the top curve.

γ_{sc}, and scattering due to the tunnelling, γ_{inc}, and can be expressed as $\gamma = \gamma_{sc} + \gamma_{inc}$. We define the tunnelling as almost coherent when γ_{sc} and γ_{inc} are small relative to other energy

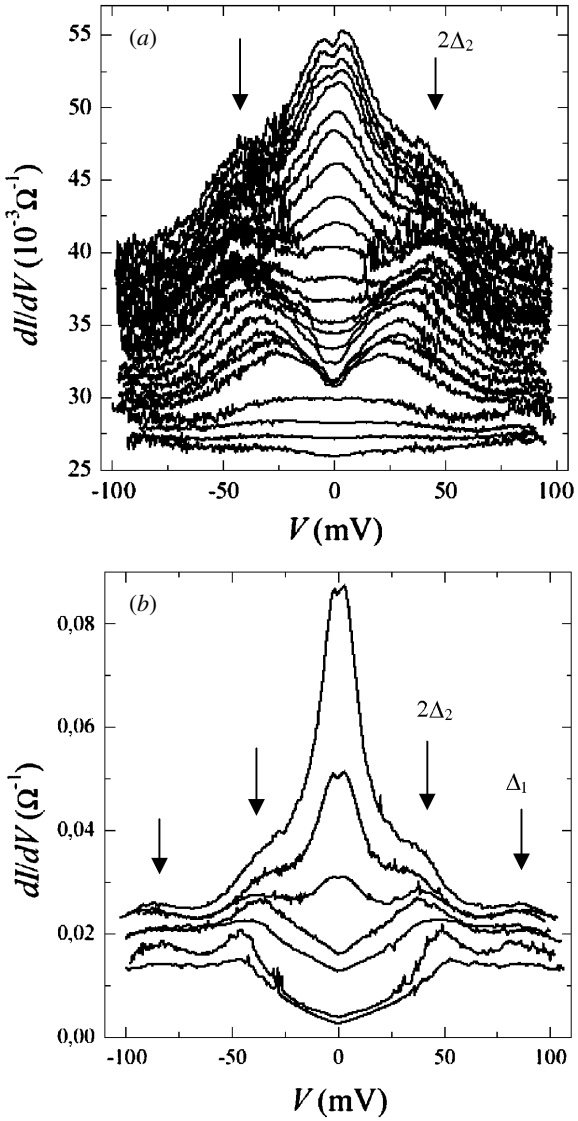

Figure 5. Spectra of $NbSe_3$–$NbSe_3$ point contacts oriented along the a^*-axis: (*a*) temperature evolution in the range 3.3–61.5 K, (*b*) spectra variation for point contacts of different quality at 4.2 K.

parameters of the electron system. In our case such parameters are the Peierls gap and the width of the electron band in the pockets. The expression for dynamic conductivity has the form

$$\frac{\sigma(V)}{\sigma(0)} = 4\gamma^2 \frac{4\gamma^2 - e^2V^2}{(e^2V^2 + 4\gamma^2)^2}. \tag{2}$$

One can see that the dynamic conductivity shows a peak at $V = 0$ with the width $\sim\gamma$ and becomes negative at $eV > 2\gamma$, indicating the instability at these voltages. Based on the known data for mobility $\mu = e/(v_{sc}\, m^*) \approx 4 \times 10^4$ cm^2 (V s)$^{-1}$ [13] and effective mass $m^* = 0.24\, m_e$ [14] we get the estimate for the intralayer scattering $\gamma_{sc} = 0.13$ meV. For a stack of $N = 30$

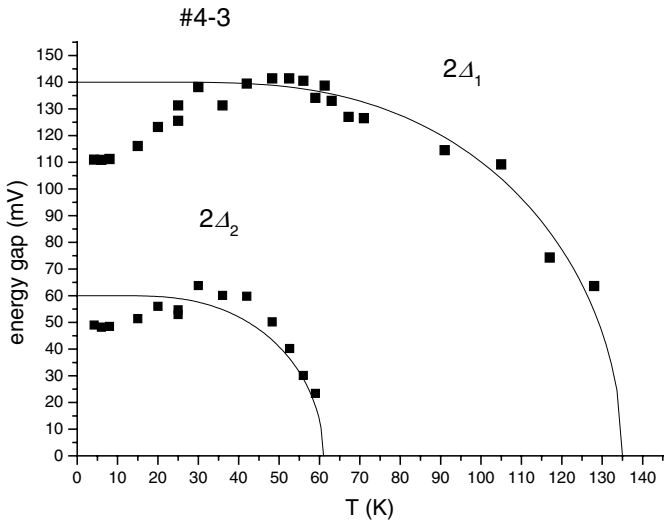

Figure 6. Fit of temperature dependences of both double gap peaks of the stack #4-3 to the BCS theory.

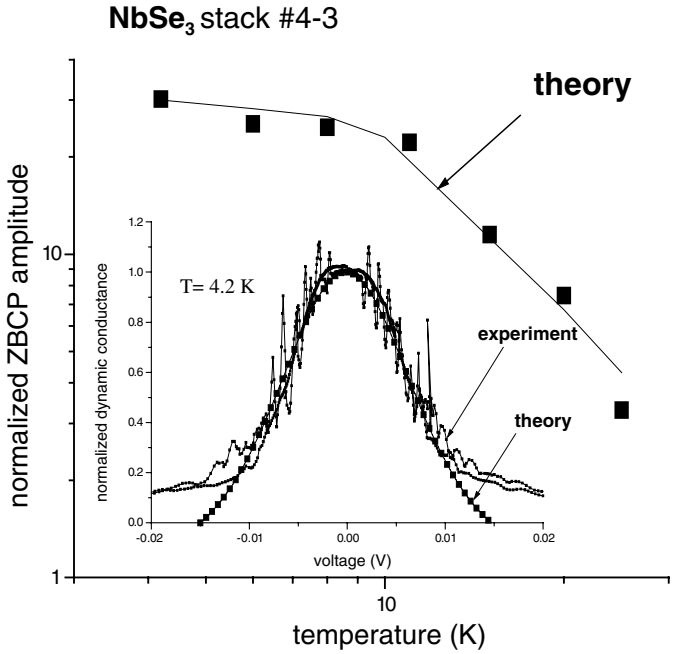

Figure 7. Fit of the temperature dependence of the ZBCP amplitude (normalized to its value above T_{p2}) to equation (1) (solid line) using the known temperature dependence of mobility in $NbSe_3$ [13]. The inset shows the fit of the experimental shape of ZBCP to equation (2).

junctions that gives a half-width of ZBCP $\gamma_{\rm eff} = N\gamma \approx 4$ mV. That is about half that observed experimentally for the samples of best quality.

Next we compare the shape of experimental ZBCP of sample #4-3 with that given by equation (2) using γ as a fitting parameter. The inset to figure 7 shows a very nice fit to the

theory for effective γ-parameter $\gamma_{\rm eff} = 7.5$ mV. For $N = 30$ that gives $\gamma = 0.25$ mV, and we can conclude that for our best samples at low temperatures the criterion of coherent tunnelling $\gamma/\Delta \ll 1$ [7] holds quite well, $\gamma/\Delta = 0.1$. Using the previous estimate for $\gamma_{\rm sc}$, $\gamma_{\rm sc} = 0.13$ mV, we can also conclude that the contribution of scattering due to the tunnelling is small enough $\gamma_{\rm inc} = 0.12$ mV and the ratio $\Gamma = \gamma_{\rm inc}/\gamma_{\rm sc} \approx 1$ at low temperatures.

We can independently extract this ratio analysing temperature dependence of the ZBCP amplitude. As can be seen from equation (1), the temperature dependence of the ZBCP amplitude is determined only by the value of γ, $\sigma(0, T) \propto 1/\gamma = [e\hbar/\mu(T)m^* + \gamma_{\rm inc}]^{-1}$.

We fit this dependence to the experimental temperature dependence of the ZBCP amplitude assuming that $\gamma_{\rm inc}$ is temperature independent and using the known temperature dependence of the in-plane $\mu(T)$ dependence [13]. In this fit we used $\Gamma(4.2\ {\rm K})$ as a fitting parameter. By variation of Γ we found the best fit for $\Gamma = 1$ (figure 7). That is consistent with the value of Γ found from the fit of ZBCP shape to the theory. Another important point is that theoretical temperature dependence reproduces the saturation of ZBCP amplitude at low temperatures. That results from saturation of $\mu(T)$ at $T \to 0$.

Thus we can conclude that for high quality $NbSe_3$ stacks ZBCP is quantitatively and self-consistently described by the model of coherent interlayer tunnelling of pocket carriers. Smearing out of ZBCP with temperature can be naturally explained by an increase of intralayer scattering with T while suppression of ZBCP on structures of poor quality at low temperatures is caused by an increase of scattering in the tunnelling channel. In both cases the increase of γ eventually leads to a transition to the incoherent tunnelling regime that is characterized by tunnelling type of spectra at low biases.

The value of $\gamma_{\rm sc}$ may be also effectively changed by a magnetic field. At low temperatures we observed a transition from ZBCP to the tunnelling regime induced by $B//a^*$ (see the next section). In support of our conclusion that ZBCP is a result of coherent tunnelling we can also argue that ZBCP has never been observed by methods of incoherent tunnelling such as STM [10] or N-CDW point contact spectroscopy [15].

We consider the gap structures to be related to the quasiparticle tunnelling over the CDW gap when the bias voltage reaches and exceeds $2\Delta_{1,2}$. In this picture, we suggest that most of the voltage drops on some weakest intrinsic junction, while the others still remain in the highly conducting state of coherent interlayer tunnelling. Sometimes the periodic structure $2n\Delta_2$ was observed with $n = \pm1, \pm2, \pm3$ [7]. That corresponds to subsequent transition of intrinsic junctions one by one into the regime of overgap quasiparticle tunnelling. Sometimes the structure was also observed with higher order of n, with $n = \pm2$ or $n = \pm3$ while lower orders were missed. That corresponds to the case when two or three neighbour intrinsic junctions switch in the quasiparticle tunnelling regime simultaneously. In both cases an observation of high order peaks at $V = n2\Delta$ implies again that n intrinsic junctions are in the quasiparticle tunnelling regime while the other $N - n$ junctions remain in the highly conducting regime of coherent tunnelling. This situation resembles a discrete multi-step transition from the regime of Josephson tunnelling to the regime of quasiparticle tunnelling in the stacked junctions of Bi-2212 high-temperature superconductor [1, 16]. In fact, when we observed a high order n for lower CDW the same order was also observed for upper CDW. For upper CDW only, however, odd high order structure $n\Delta_1$ is more often observed. That means that the carriers not condensed into lower CDW can tunnel as normal carriers for the upper CDW[9].

[9] The peak of dynamic tunnelling conductance at $eV = \Delta$, where Δ is the superconducting gap, is well known for N/I/S structures with N normal metal, I an insulator and S a superconductor. A similar peak at $eV = \Delta_1$ has also been observed in the N/I/CDW-type junctions [15].

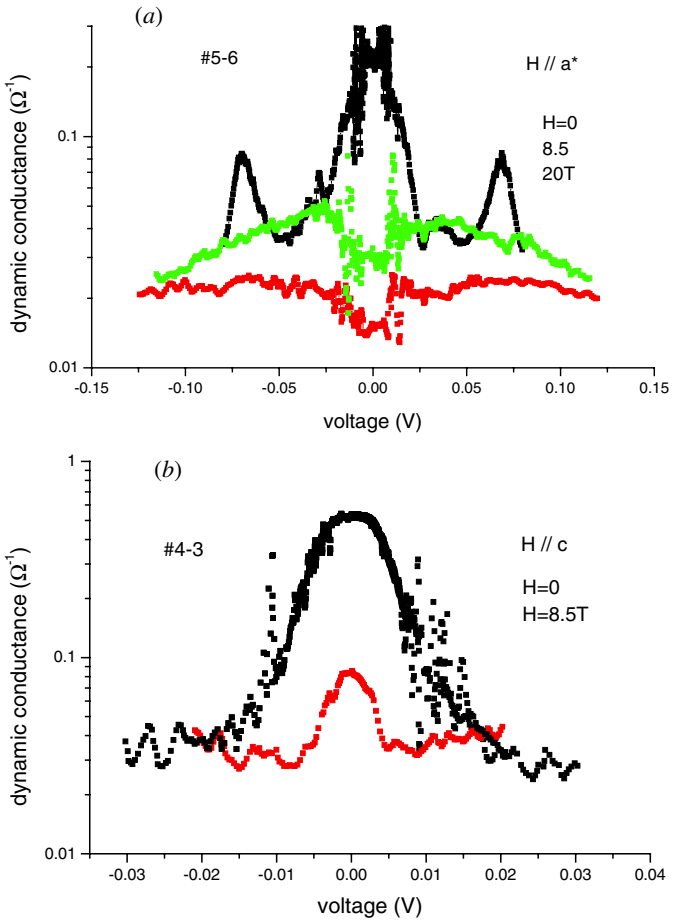

Figure 8. Interlayer tunnelling spectra variation in magnetic fields perpendicular to the conducting layers, $H//a^*$ (*a*) and parallel to the conducting layers, $H//c$ (*b*).

For the point contacts $NbSe_3$–$NbSe_3$ oriented along the a^*-axis we observed only first order gap structures at $eV = \pm 2\Delta_2, \pm\Delta_1$. That implies that the interface always plays the role of the weakest junction.

5. Influence of magnetic field on ZBCP

Generally, moderate magnetic field does not affect tunnelling conductivity in the usual case of incoherent tunnelling (see e.g. [17]). The case of coherent tunnelling was studied only in the case of layered high-T_c materials [18, 19], where the presence of vortices changes dramatically the quasiparticle properties. In our case vortices are absent. We studied the effect of magnetic field on ZBCP and found as preliminary results that ZBCP is rather sensitive to magnetic field and its orientation. ZBCP evolution in fields of two orientations, perpendicular ($H//a^*$) and parallel ($H//c$) to the conducting layers is shown in figure 8. One can see that the perpendicular field affects ZBCP in a very similar way as temperature: ZBCP broadens and the gap opens at small bias voltages (compare spectra at $H = 0$, 8.5 T, 20 T in figure 8(*a*) with spectra at 6 K, 30 K, 42 K in figure 4(*b*)). The parallel field affects ZBCP in a different way: ZBCP narrows and its amplitude decreases (figure 8(*b*)).

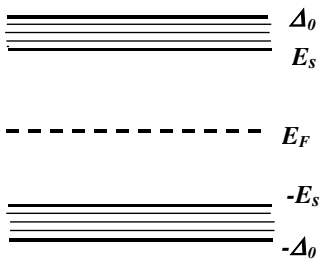

Figure 9. Schematic view of the energy spectrum of a CDW conductor with amplitude soliton states.

In the case of a perpendicular magnetic field we do not anticipate any change in the interlayer tunnelling because quasiparticle wavefunctions remain similar in all layers. However, a perpendicular field increases the intralayer energy of quasiparticles in the ungapped pockets (due to Landay quantization of electron levels in magnetic fields) and hence diminishes the CDW gap. This occurs when the Larmor radius becomes comparable with the CDW coherence length, i.e. in fields $H \sim 2\pi^2 c/\left(eh\Delta_2^2 v_F^2\right)$, where v_F is the Fermi velocity. At $\Delta_2 \sim 30$ meV and $v_F \sim 10^8$ cm s^{-1} we estimate a strong effect of the magnetic fields $H > 4$ T. Increase of the quasiparticle concentration leads to enhancement of the scattering rate γ due to their interaction. As a result, the peak at zero voltage drops. In this scenario the perpendicular magnetic field acts similar to the temperature.

A parallel field can hardly change the in-plane momentum. Its effect on ZBCP might be rather related to the abolition of pockets by the field [20] or by the shift of typical pocket momenta in neighbouring layers as described in [18]. This shift leads to suppression of the amplitude of coherent tunnelling.

6. Probing of the states localized inside the CDW gap

Theoretically, a major peculiarity of electronic properties of CDWs is that free electrons near the gap edge Δ_0 are not stable with respect to the deep self-trapping towards the midgap states which are provided by a formation of so-called amplitude solitons (see e.g. [21, 22] and references therein). The electronic energy gain Δ_0 is partly compensated by the energy of the CDW amplitude distortion $\Delta_0 th(x/\xi_0)$ and equilibrates at the total energy of the soliton $E_s = 2\Delta_0/\pi$ that is less than Δ_0 by $\approx\frac{1}{3}\Delta_0$. The schematic picture of energy states, shown in figure 9, suggests a possibility of observing a lower threshold for the tunnelling conductivity when the bias energy exceeds E_s. The existence of amplitude solitons has been well documented in dimeric CDW materials such as polyacetylene or $CuGeO_3$. However, for materials with sliding CDW, that is incommensurate or higher order commensurability (MX_3 with M—Ta, Nb, X—S, Se; $K_{0.3}MoO_3$; etc), the existence of amplitude solitons has not been reliably demonstrated yet. Here we report our preliminary results on observation of the subgap states by interlayer tunnelling in the lower CDW state of $NbSe_3$.

As was discussed above, at low temperatures the subgap part of interlayer spectra is masked by the zero bias conductance peak. However, ZBCP can be effectively suppressed by a magnetic field perpendicular to the layers or by temperature increase above 25 K. In both cases we found the presence of the subgap structure that is characterized by a sharp increase in tunnelling conductance with bias voltage exceeding some threshold energy localized inside the gap.

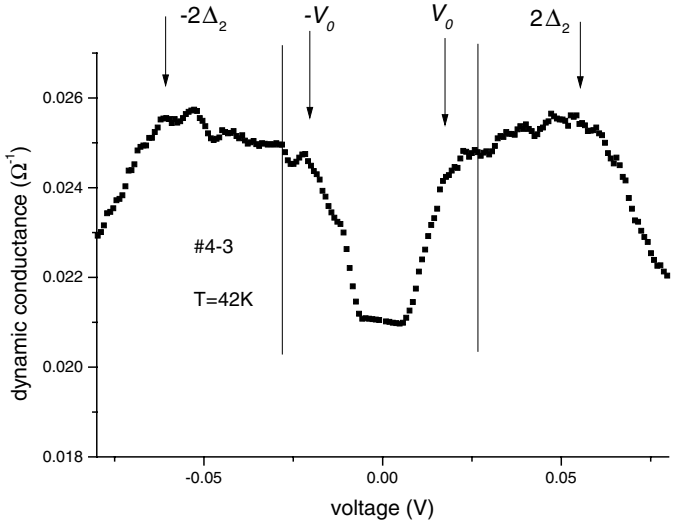

Figure 10. Interlayer tunnelling spectrum of stack #4-3 at 42 K. Arrows mark the double gap structure $\pm 2\Delta_2$ and the broad peak inside the gap $\pm V_0$. The gap edge position at $V = \pm\Delta_2$ is marked by vertical lines.

A typical spectrum of that type is shown in figure 10. As was shown before, the broad maxima at $|V| \approx 60$ mV can be identified as $|eV| \approx 2\Delta_2$. Then we can easily find the bias voltage corresponding to the edge of the gap $|eV| = \Delta_2$, that is shown by vertical lines. Now one can see that threshold voltage V_t lies well below the gap edge. Above V_t tunnelling conductance grows rapidly and reaches a broad maximum at V_0. We can suggest that the maximum point corresponds to the local maximum of density of states inside the gap[10]. It would then be reasonable to identify that voltage with the energy level of amplitude solitons broadened by thermal fluctuations or some other factor. Indeed, from the experiment it directly follows that $eV_0 = 0.64\Delta_2$ which is remarkably close to the theoretical value $E_s = 2\Delta_2/\pi = 0.65\Delta_2$, $eV_0 \equiv E_s$. Similar features were found for interlayer tunnelling spectra at low temperatures when ZBCP was suppressed by high fields $H//a^*$ (see e.g. curve at 20 T in figure 8(*a*)). All these findings demonstrate the capability of the interlayer tunnelling for studies of the subgap structure as well. Systematic studies of the subgap structure will be published elsewhere. Here we only mention that the structure is well reproduced on many samples and that the ratio $2\Delta_2/V_0$ appears to be temperature independent and close to π.

Amplitude solitons are the lowest energy single electronic states of 1D CDWs. They are supposed to exist in the incommensurate case, and also to be compatible with any even order commensurability which is invariant under changing sign of the order parameter. Concerning the peak assignment, certainly there may be other intragap features, e.g. from impurity states as in usual semiconductors. But in the experiments presented it seems to be a generic feature, also the energy is encouragingly close to the expected theoretical value.

7. Conclusions

By using the method of interlayer tunnelling we studied the lower CDW state in $NbSe_3$. We found that the zero bias conductance peak found recently at low temperatures can be

[10] In this picture we suggest that there is some population of uncondensed (pocket) carriers in a narrow band near the Fermi surface. They can contribute to tunnelling conductivity when $eV \approx E_s$.

self-consistently described by the theory of coherent tunnelling of pocket carriers. We found considerable influence of magnetic field on ZBCP that is dependent on field orientation. We demonstrated the capability of the interlayer tunnelling method for spectroscopy of the CDW gap and the states inside the gap.

Acknowledgments

We acknowledge S I Matveenko for fruitful discussions. This work was supported by the Russian Foundation for Basic Research (project nos 02-02-17263, 01-02-16321 and 00-02-22000 CNRS), the state program 'Physics of Solid Nanostructures' (project no 97-1052), the NWO Russian–Netherlands Project, grant INTAS-01-0474, and grant CRDF No RP1-2397-MO-02.

References

[1] Kleiner R, Steimeyer F, Kunkel G and Müller P 1992 *Phys. Rev. Lett.* **68** 2394
Kleiner R and Müller P 1994 *Phys. Rev.* B **49** 1327
[2] Tanabe K *et al* 1996 *Phys. Rev.* B **53** 9348
[3] Krasnov V M *et al* 2000 *Phys. Rev. Lett.* **84** 5860
Suzuki M and Watanabe T 2000 *Phys. Rev. Lett.* **85** 4787
[4] Latyshev Yu I, Yamashita T and Bulaevskii L N *et al* 1999 *Phys. Rev. Lett.* **82** 5345
[5] Heim S and Nachtrab *et al* 2002 *Physica* C **367** 348
Nachtrab T, Heim S, Mößle M, Kleiner R, Waldmann O, Koch R, Müller P, Kimura T and Tokura Y 2002 *Phys. Rev.* B **65** 012 410
[6] Latyshev Yu I and Monceau P *et al* 1999 *J. Phys. IV France* **9** Pr 10–165
[7] Latyshev Yu I, Sinchenko A A and Bulaevskii L N *et al* 2002 *JETP Lett.* **75** 93
[8] Kim S-J, Latyshev Yu I and Yamashita T 1999 *Supercond. Sci. Technol.* **12** 728
[9] Ong N P and Brill J W 1978 *Phys. Rev.* B **18** 5625
[10] Dai Z *et al* 1992 *Phys. Rev.* B **45** 9469
Xue Q *et al* 1993 *Phys. Rev.* B **48** 1986
[11] Latyshev Yu I, Kim S-J and Yamashita T 1999 *JETP Lett.* **69** 84
[12] Krasnov V M, Yurgens A, Winkler D and Delsing P 2001 *Preprint* cond-mat/0101241
[13] Ong N P 1978 *Phys. Rev.* B **18** 5272
[14] Coleman R V *et al* 1990 *Phys. Rev.* B **41** 460
[15] Sinchenko A A, Latyshev Yu I, Zybtsev S G, Gorlova I G and Monceau P 1999 *Phys. Rev.* B **60** 4624
Sinchenko A A, Latyshev Yu I, Pokrovskii V Ya, Zybtsev S G and Monceau P 2003 *J. Phys. A.: Math. Gen* **36** 9311–22
[16] Kleiner R, Müller P, Kohlstedt H, Pedersen N F and Sakai S 1994 *Phys. Rev.* B **50** 3942
[17] Wolf E L 1985 *Principles of Electron Tunneling Spectroscopy* (New York/Oxford: Oxford University Press/ Clarendon)
[18] Bulaevskii L N, Graf M J and Maley M P 1999 *Phys. Rev. Lett.* **83** 388
[19] Morozov N, Krusin-Elbaum L, Shibauchi T, Bulaevskii L N, Maley M P, Latyshev Yu I and Yamashita T 2000 *Phys. Rev. Lett.* **84** 1784
[20] Balseiro C A and Falicov L M 1985 *Phys. Rev. Lett.* **55** 2336
Balseiro C A and Falicov L M 1986 *Phys. Rev.* B **34** 863
[21] Brazovskii S A 1980 *Sov. Phys.–JETP* **51** 342
[22] Matveenko S I and Brazovskii S A 2002 *Phys. Rev.* B **65** 245 108
Brazovskii S A and Matveenko S I 2002 *Preprint* cond-mat/0208121